https://doi.org/10.5194/egusphere-2026-3337
Preprint. Discussion started: 16 July 2026

Modelling dynamic coastal vegetation establishment and ecosystem engineering in hydro-morphodynamic models with DYCOVE

Nelson Tull[1,2] and Muriel Z.M. Brückner[1,2]

[1]Department of Civil & Environmental Engineering, Louisiana State University, Baton Rouge, 70803, USA
[2]Center for Computation and Technology, Louisiana State University, Baton Rouge, 70803, USA

Correspondence to: mbruckner@lsu.edu

Abstract. Coastal areas are complex environments with diverse hydrodynamic, morphological, sedimentological, and biological contexts. Vegetation is increasingly recognized as a crucial agent that shapes the geomorphology and hydrology of coastal and riverine systems by inducing a hydraulic roughness that influences flow velocities, inundation, erosion, and deposition. At the same time, vegetation growth depends on the environmental habitat conditions, which it modifies continuously, resulting in a biophysical feedback-loop. This loop between plant growth and the physical environment is inherently dynamic, meaning they both vary spatiotemporally through their interactions; however, these dynamics are currently excluded from most hydro-morphodynamic models that predict long-term coastal change. We present the DYnamic COastal VEgetation model DYCOVE: an open-source, process-based vegetation model that simulates dynamic coastal marsh vegetation by representing key ecological processes such as seed dispersal, establishment criteria, growth curves, and mortality rules. Vegetation dynamics are governed by species-specific thresholds for inundation, desiccation, bed level change, and flow conditions while age-dependent stress tolerance enables realistic transitions from seedlings to mature plants of multiple species. Based on literature-derived parameterizations of ecological thresholds, DYCOVE reproduces realistic vegetation distributions and zonations both in tidally- and fluvially-impacted coastal environments with an F1 score above 0.8 and species distribution with a total accuracy of 70%. DYCOVE's flexible, species-agnostic framework allows exploration of how various vegetation types influence coastal hydrodynamics, sediment transport, and land-building, representing a crucial advancement in process-based eco-hydro(morpho)dynamic modelling.

Summary. Coastal vegetation both responds to and actively shapes coastlines through dynamic interactions. DYCOVE can predict vegetation via establishment, growth, aging, and mortality in a variety of coastal environments. Coupled with coastal physics-based models, it simulates vegetation dynamics with strong predictive skill, enabling assessment of feedbacks between vegetation and the earth surface, species distributions, and invasive species impacts under changing environmental conditions.

https://doi.org/10.5194/egusphere-2026-3337
Preprint. Discussion started: 16 July 2026

1 Introduction

Coastal areas and wetlands are complex environments with diverse hydrodynamic, morphological, sedimentological, and biological contexts. Coastlines are hotspots of settlements with dense populations since the Holocene and provide important services and ecosystem benefits that are crucial for economic, social, and cultural welfare of coastal populations (Costanza et al., 1997; Barbier et al., 2011; Batker et al. 2014). Many middle- and high-latitude coastlines are fringed by marshes, particularly saltmarshes, which are highly productive ecosystems rich in biodiversity, consisting of a variety of plant species that provide important habitats for a wealth of fauna (Day et al., 2013). Saltmarshes are further recognised as important carbon sinks that protect coastal areas from the effects of natural disasters, such as erosion and storm surges (Temmerman et al., 2023; Day et al., 2024).

Saltmarsh communities organize in distinct zonations along inundation and salinity gradients linked to flood and osmosis stresses that determine habitat suitability (Friedrichs & Perry, 2001). Marshes can be highly dynamic as they are prone to erosion but also rapidly colonize new sediments. Their distribution is not only influenced by but also influences local physical processes and geomorphology including topography and creek patterns (Adam, 1990). Through ecosystem engineering effects, they mediate flow and sediment transport patterns, bind sediment with their roots, trap sediments, and produce soil through biomass production (Nyman et al., 1993; Jones et al., 1994; Sasser et al. 2018). Species composition and marsh type vary regionally and in time (Fischer et al., 2000), and their species-specific traits were demonstrated to alter ecosystem engineering effects that determine channel network initiation and shape, tidal morphology, and broader landscape form (Brückner et al., 2019; Bij de Vaate et al., 2020; Schwarz et al. 2018; Cornacchia et al., 2024). Specifically, ecological processes such as colonization, growth strategies and timing, species competition, life-cycles, and seasonal biomass production affect their distribution, adaptability to stresses, and ecosystem engineering capacity (e.g., Schwarz et al., 2018; Schwarz et al., 2020; Cassaway et al., 2024; Wei et al., 2025).

Most coastal models that assess decadal or long-term coastal dynamics typically lack these vegetation dynamics; instead, vegetation is most commonly represented by constant or static hydraulic roughness or cohesivity parameters (e.g., Piercy et al., 2022). Few models exist that couple physics-based and ecological models interactively at timescales that resolve spatial and temporal ecological processes, such as vegetation growth, mortality, and seasonality (e.g., Brückner et al., 2019; Schwarz et al., 2020; Finotello et al., 2022; Gourgue et al., 2024; Dzimballah et al., 2025), but those are either limited to a single-species and environment, not open-source, or lack documentation that allows for the broader application in the ecohydraulic and ecomorphodynamic modelling community.

Here we present an open-source process-based, dynamic vegetation model called the DYnamic COastal VEgetation (DYCOVE) model that is implemented as a Python package, enabling straightforward installation via standard package management tools. DYCOVE is based on a vegetation model presented and applied in Brückner et al. (2019), Brückner et al. (2020), and Bij de Vaate et al. (2020) that has been extended from these previous applications to represent dynamic vegetation growth of multiple marsh species in both tidal and deltaic environments. It is coupled with two sophisticated

https://doi.org/10.5194/egusphere-2026-3337
Preprint. Discussion started: 16 July 2026

physics-based software packages that are used worldwide for process-based coastal modelling: Delft3D Flexible Mesh and ANUGA. By integrating DYCOVE into these numerical models, detailed vegetation life-cycles and biophysical interactions can be integrated into the physical and empirical equations to model coastal change (Fig. 1a). DYCOVE was developed with the purpose to help advance coastal vegetation modelling beyond the use of constant or static vegetation roughness by supplying a state-of-the-art open-source framework that is freely available and well-documented.

To illustrate the capabilities of DYCOVE, we present two sets of test cases: one application in a synthetic, exploratory macrotidal flat model using the hydro-morphodynamic software Delft3D Flexible Mesh and one application on a realistic topo-bathymetry of a microtidal, river-dominated delta model using ANUGA. In our case studies, we reproduce vegetation establishment and spatio-temporal patterns of vegetation and channel development, showing that DYCOVE can reproduce marsh species pattern and dynamics based on literature-derived vegetation parameterizations across tidally and fluvially-driven environments, including species changes linked with species invasions. These capabilities make DYCOVE suitable for capturing self-organized vegetation and morphological patterns that naturally develop from complex, nonlinear feedbacks between flow, sediment transport, landform evolution, and vegetation dynamics (Murray et al., 2008; Coco et al., 2013; Cornacchia et al., 2024).

2 Methodology

DYCOVE is a process-based vegetation model developed from a dynamic saltmarsh vegetation model described in Brückner et al. (2019) that couples dynamic saltmarsh vegetation with Delft3D FLOW, the precursor of Delft3D Flexible Mesh (DFM) (Deltares, 2025). Based on a previous dynamic vegetation model for riparian vegetation (van Oorschot et al., 2016), this eco-morphodynamic model reproduces tidal marsh vegetation patterns and dynamics in conjunction with the hydro-morphodynamics in estuaries. The Brückner-model has several disadvantages: first, it was coupled offline with Delft3D FLOW, making computations slow due to large file exchanges; second, it relies on the proprietary MATLAB software. The aim of DYCOVE is to provide an open-source model for dynamic marsh vegetation processes and resulting hydraulic roughness that is coupled with the widely used software packages ANUGA and DFM. The ANUGA (Australia National University and Geoscience Australia) model is an open-source hydrodynamic model that solves the shallow-water equations on unstructured computational meshes using a finite volume solver (Mungkasi et al., 2013). ANUGA is freely available, easy to install, and written in Python, which allows straightforward integration of the Python-based DYCOVE. DFM is a widely used hydro-morphodynamic (H-M) model that solves the shallow-water equations and computes empirical sediment transport and morphodynamic changes via the Exner equation (Deltares, 2025). Like ANUGA, DFM uses an unstructured computational mesh (many grid types are supported) with a finite volume solver. DFM is primarily written in Fortran, requiring the use of a Basic Modeling Interface (BMI; Hutten et al., 2020; Baart et al., 2022) to integrate DYCOVE. DYCOVE does not contain its own BMI, but coupling with additional H-M models is straightforward if they can be run and accessed via Python.

https://doi.org/10.5194/egusphere-2026-3337
Preprint. Discussion started: 16 July 2026

DYCOVE can be widely applied to study the bidirectional effects of coastal vegetation and hydro-morphodynamics. Example applications include analysing the response of vegetation dynamics and geomorphology to changes in hydrodynamic or sedimentary forcing based on vegetation characteristics, how vegetation traits and life-cycles determine landscape evolution, and the implementation of restoration strategies and management practices. As DYCOVE can model multiple vegetation species in a single simulation, users may also model species zonation, transitions, and invasions and their feedbacks with physical coastal processes.

2.1 Modelling concept and process equations

In brief, DYCOVE predicts vegetation cover using a fractions approach, meaning that vegetation is allocated to grid cells via vegetation fractions based on habitat suitability governed by inundation period, desiccation period, and flow velocity (causing uprooting) thresholds, and in case of morphodynamic computations, by erosion and burial depths. DYCOVE computes a hydraulic roughness based on vegetation cover in each grid cell that is directly incorporated into the shallow-water and, if applicable, sediment transport equations. Hydraulic roughness is hereby based on the sum of all vegetation fractions and their dimensions, such as stem height, diameter, and density, and each individual grid cell can host any number of vegetation fractions (Baptist, 2007; Deltares, 2025) (Fig. 1).

DYCOVE uses the output of the H-M model to allocate vegetation via detailed ecological rules, including seed dispersal, seedling establishment, growth, aging, stress tolerance, and mortality (Fig. 1). The allocated vegetation cover is then translated into a hydraulic roughness for each computational grid cell and used in the H-M model. At regular coupling intervals (Ecological timesteps; ETS), vegetation is updated based on the defined colonization rules, growth curves, mortality functions. The ecological rules and functions in DYCOVE depend on user-defined parameters that can be informed from values in the literature or measurements. In Sects. 2.1.1 to 2.1.4, the rules and functions implemented in DYCOVE are outlined in more detail.

https://doi.org/10.5194/egusphere-2026-3337
Preprint. Discussion started: 16 July 2026

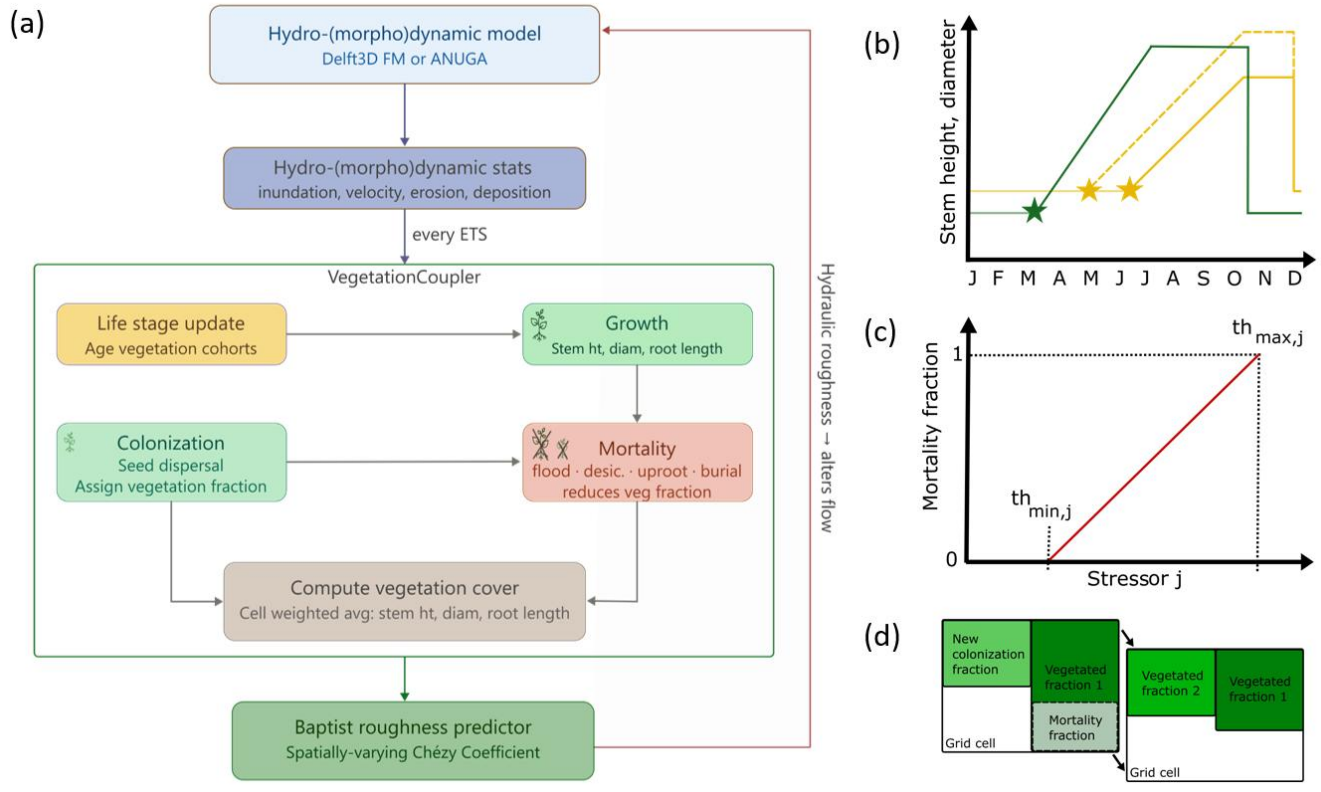

Figure 1: A) Conceptual figure of DYCOVE and coupling with hydro-(morpho)dynamic (H-M) models. Every ecological timestep (ETS), vegetation is predicted based on the output of the H-M model and the colonization and mortality characteristics of the vegetation species. The resulting hydraulic roughness is fed back into the HM model. Life-cycle characteristics control vegetation growth and resistance to mortality. B) Example annual growth curves of two species (yellow and green). Yellow dashed and solid lines describe the same species with two colonization events that occur during successive timesteps (stars). Letters denote months. C) Linear mortality function based on the stresses j (inundation period, desiccation period, and flow velocity). Minimum and maximum mortality thresholds, $th_{min,j}$ and $th_{max,j}$, are user-defined for each species, life-stage, and stressor. D) Example of how vegetation is allocated and removed from a computational grid cell with a new colonization fraction being added to the existing vegetation fraction (dark green). Mortality is calculated for each existing fraction and removed from the cell. Note that each vegetated fraction has different properties based on age and/or species properties.

2.1.1 Vegetation colonization

Vegetation colonization occurs at user-defined time-steps and occurs every simulated year (Fig. 1b). Several colonization time-steps each year are possible and are independent of the growth period (i.e., growth will end at the same time each year regardless of when colonization events occurred). Colonization is specified by an initial colonization fraction between 0-1 (Fig. 1d) that is user-defined and constant for each vegetation species. The colonization fraction is assigned an initial stem height, root length, and stem diameter. If multiple colonization time-steps are defined (either per species or among several species), each grid cell is colonized until a total carrying capacity fraction of 1 is reached.

If the colonized area is suitable, vegetation can establish and start growing. Suitable grid cells for colonization are selected via one of four different seedling dispersal strategies, each based on hydrodynamic conditions present during the previous

https://doi.org/10.5194/egusphere-2026-3337
Preprint. Discussion started: 16 July 2026

coupling period: (1) cells that were partially wet and partially dry for any length of time (intertidal elevations), (2) wet or partially wet cells (sub- and intertidal elevations), (3) dry or partially dry cells (inter- and supratidal elevations), and (4) all grid cells. The model by Brückner et al. (2019) was developed for environments where vegetation growth is predominantly driven by the tides, such as in macro- and meso-tidal estuaries and coastlines, and only provides colonization strategy (1). We implemented the three additional options to overcome two colonization limitations. First, in coastal areas where flooding is impacted by intermittent fluvial flooding, such as river deltas, colonization may be underpredicted if the flood extent during the colonization window is smaller than average due to unsteady river discharge. This can be overcome by colonizing additional areas in the supra- or subtidal zones (see also Sect. 3.2 as an example). Second, when using existing well-developed morphologies based on topographic data, high elevations that are located outside the typical flood range will be left bare under colonization strategy (1). Strategies (3) or (4) allow adding vegetation at these high elevations. Since the model is mortality driven, any cells that are colonized outside the habitat range will be 'killed' and removed instantaneously (removing falsely-colonized vegetation in open water, for example). Importantly, the vegetation will be removed before coupling with the H-M model. The user can also apply quasi-random colonization by setting an establishment probability per vegetation species. This scheme selects a random number of cells from the suitable colonization area (e.g., P_{est} = 0.2 selects 20% of all suitable cells for vegetation colonization (Bij de Vaate et al., 2020).

2.1.2 Vegetation growth and aging

Once established, a vegetation fraction grows linearly with time in stem height and diameter, and in root length. Annual stem height growth is defined for three seasons (Fig. 1b): 1) a spring growth rate from an initial to a maximum stem height, 2) a phase of constant summer stem height after the growth season, and 3) a winter stem height if aboveground biomass dies off in winter. The user can specify the growth, summer, and winter period freely per modelled species, allowing for staggered growth curves for different species. If no seasonality is desired, a constant stem height can be enforced by setting the initial, summer and winter stem height to the same value.

Vegetation has a maximum life span after which it dies of senescence. This lifetime can be split into several life-stages that represent seedling and more mature stages in the plant's life-cycle (van Oorschot et al., 2016). The seasonal growth cycle described above can be defined for each life-stage and the user can set different summer and winter stem height for each life-stage separately.

Stem diameter and root length grow linearly from the initial to the final value at the end of the life span of the vegetation. Stem density is constant for each life-stage; instead, vegetation cover is controlled by vegetation fractions, which are determined by the colonization and mortality routines.

2.1.3 Vegetation mortality and stresses

The vegetation cover (via fractions) in DYCOVE is primarily driven by mortality, where newly colonized vegetation is removed instantaneously if the habitat is not suitable based on the defined habitat thresholds. Vegetation mortality is induced

https://doi.org/10.5194/egusphere-2026-3337
Preprint. Discussion started: 16 July 2026

by environmental stressors—including prolonged inundation, desiccation, high flow velocities, and high net erosion or deposition. These stressors can induce partial or complete mortality based on mortality thresholds defined by the user (Fig. 1c) and are typically informed by the literature. If a stressor exceeds the lower mortality threshold defined for a given species during a given coupling interval, a fraction of the vegetation is removed from the computational grid cell based on a linear mortality function (Fig. 1d). Hereby, the mortality fraction depends linearly on the strength of the stressor and is multiplied by the initial vegetation fraction at colonization. The mortality fraction is unity if the upper mortality threshold is exceeded. If several environmental stressors cause mortality, the total mortality is the sum of all mortality fractions. If several vegetation fractions are present in a grid cell, the mortality fraction is computed and removed for each fraction individually. The lower and upper mortality thresholds are defined per vegetation species, life-stage, and stressor.

Importantly, vegetation tolerance to stress can increase with plant age, e.g., at the transition from seedling to mature plant, which can be represented via the life-stages. This age-dependent behaviour allows DYCOVE to capture successional dynamics that are typically absent from available eco-morphodynamic models.

A vegetation fraction is removed completely once its maximum life span is reached. This capability allows for the representation of both annual and perennial vegetation or vegetation with varying life cycle lengths.

2.1.4 Competition and multiple vegetation species

DYCOVE's parameterization is intentionally species-agnostic, enabling simulations of individual species as well as mixed vegetation assemblages with varying traits. This flexibility provides opportunities to test how differences in colonization strategies, growth rates, and resistance to disturbance influence species distributions and resulting ecosystem engineering effects, a capability that was shown to be important for assessing tidal channel development (Schwarz et al., 2020; Cornacchia et al., 2024). Species allocation in DYCOVE is sequential with the user defining the order of colonization of each species, which incorporates competition for space. Due to the maximum carrying capacity per cell of a total vegetation fraction of unity, a species that colonizes early with high colonization fractions can fill grid cells before the colonization window of a later species occurs. If colonization of several species occurs in the same timestep, the user can define the order at which each species is called to incorporate competition for space directly. Direct competition for light or nutrients is currently not supported in DYCOVE.

2.2 Coupling with physics-based hydro-morphodynamic models

Both supported physics-based models (DFM and ANUGA) solve the shallow-water equations to simulate flow based on conservation of mass and momentum in three dimensions. Although three-dimensional flow can be solved, DYCOVE is currently designed to be coupled to depth-averaged, one- or two-dimensional simulations, which is sufficient for most coastal modelling applications. More complex three-dimensional vegetation feedbacks that might require a more sophisticated representation of vertical vegetation area and phenology are not supported. DFM solves empirical sediment transport and morphological change whereas ANUGA is a purely hydrodynamic model. However, recent work has coupled

https://doi.org/10.5194/egusphere-2026-3337
Preprint. Discussion started: 16 July 2026

ANUGA with the particle-tracking package *dorado* (Hariharan et al., 2020), which models particle flow paths and residence times for particles with a range of densities (Wright et al. 2022).

Vegetation distributions can be updated at user-specified coupling intervals that can be on the order of several days or weeks, allowing seasonal variability in establishment, growth, and mortality to interact with transient hydrodynamic forcing such as spring floods, tidal anomalies, and storm periods. Each coupling timestep between DYCOVE and DFM or ANUGA modifies local hydraulic roughness in each computational grid cell based on vegetation properties and cover, which in turn alters flow patterns, sediment transport, and deposition, closing the feedback loop between ecological and physical processes. Each coupling interval, vegetation effects are passed to the H-M model via a spatially-varying hydraulic roughness parameter C in units $m^{1/2}/s$ following the well-known Baptist formula (Baptist, 2007) for the case of submerged vegetation:

$$C = \left(\frac{1}{C_b^2} + \frac{C_D n h_v}{2g}\right)^{-\frac{1}{2}} + \frac{\sqrt{g}}{\kappa} ln\left(\frac{h}{h_v}\right) \quad (1)$$

and for the case of emergent vegetation:

$$C = \left(\frac{1}{C_b^2} + \frac{C_D n h}{2g}\right)^{-\frac{1}{2}} \quad (2)$$

where n is the vegetation density with $n = m \cdot D$ where m is the number of stems per m^2 and D is the stem diameter in m, C_D is the drag coefficient, h_v is vegetation height and h is water depth, κ=0.41 is the von Karman constant, and C_b is the bed roughness. These equations allow for a detailed implementation of vegetation dimensions and characteristics, allowing DYCOVE to dynamically implement effects of spatio-temporal changes in vegetation structure and density into the hydro-morphodynamic computations. In grid cells that host several vegetation fractions, the vegetation properties are averaged first, weighted by their respective vegetation fractions in the cell. The average stem height and diameter, density, and drag coefficient are then passed to Eq. (1) or (2), depending on the average stem height relative to the water depth. It is worth noting that for morphodynamic simulations with DFM, an additional vegetation drag force is added to the momentum equation and the total roughness C is included in the friction term. For sediment transport, the shear stress is based on the bed roughness only (defined as C_b in Eq. (1) and (2)) to avoid unrealistic erosion in vegetated grid cells (see Deltares, 2025).

2.3 Simulation timescales

Similar to morphological changes, vegetation growth and response is slow compared to changes in hydrodynamics. We can therefore make use of an ecological acceleration factor that is based on the widely used concept of the morphological acceleration factor (MORFAC) in morphodynamic modelling (Ranasinghe et al., 2011). The MORFAC is based on the assumption that each recurring hydrodynamic forcing (e.g., a tidal cycle) will induce the same rate of change on the morphology. As a result, the net morphodynamic change caused by a number of modelled tidal cycles N, will be equal to the morphodynamic change over one tidal cycle multiplied by N. A similar assumption can be applied to ecological change;

https://doi.org/10.5194/egusphere-2026-3337
Preprint. Discussion started: 16 July 2026

vegetation will not respond instantaneously to a change in water level over minutes or hours, but rather to a continuous change in inundation or desiccation over weeks or months (Elsey-Quirk et al., 2024). This allows us to speed up the vegetation computations via an ecological acceleration factor ECOFAC (e.g., Coco et al., 2013; van Maren et al., 2015; Brückner et al. 2019). The ECOFAC is used in DYCOVE whether or not the underlying simulation includes morphology, but for simulations with morphology, the MORFAC and ECOFAC are set to the same value for simplicity.

To set the simulation timescale, the user must define a set of parameters to establish 1) the annual simulation time, 2) the coupling interval, and 3) the annual number of couplings. The coupling time-step is the hydrodynamic simulation time between vegetation updates. We call this timestep the ecological timestep (ETS). By multiplying the ETS with the ECOFAC, we establish the ecological time that this hydrodynamic interval represents. It is important that the hydrodynamic forcing in each ETS is consistent, i.e., a full instead of a partial tidal cycle, to avoid a coincidental die-off (e.g., the ETS = flood tide only). Second, the number of couplings per year n_{ets} needs to be set in a way that makes sense for a calendar year (e.g., 12 or 24, resulting in monthly or bi-weekly couplings), which determines the hydrodynamic simulation time for one year $t_{hydro,y} = n_{ets} \cdot$ ETS. To run several years, simply multiply $t_{hydro,y}$ by the number of years to obtain the total simulation time. A typical set of values for tidal systems is ETS = 12.4 hours (one M2-tidal cycle), n_{ets} = 24 and ecological acceleration factor of 30. This setting means that vegetation is coupled 24 times per ecological year, and each coupling represents 15.5 days of ecological time. Note that all vegetation computations (e.g., colonization and mortality) are based on the H-M model outputs of the previous ETS.

3 Model application and results

To test the vegetation patterns derived using DYCOVE, we present two sets of simulations. Set 1 is an exploratory tidal flat model based on estuaries in the Netherlands in DFM (Sect. 3.1). Set 2 is a hydrodynamic model in ANUGA constructed from a realistic topo-bathymetry dataset of Wax Lake Delta (WLD), a microtidal river delta in southern Louisiana, USA, that hosts typical freshwater marsh species (Sect. 3.2). The results of these simulations demonstrate that DYCOVE's process-based approach can adequately represent vegetation cover compared with observations and static vegetation thresholds derived from bed elevation relative to mean sea level, a common practice in vegetation models (Morris et al., 2016; Wright et al., 2022; Vahsen et al., 2024). For both cases we model multi-species scenarios with parameterizations based on the scientific literature (Table S1) and do qualitative and quantitative comparisons between modelled vegetation cover and observations.

3.1 Vegetation cover and dynamics in an exploratory eco-morphodynamic model in DFM

We developed an idealized tidal flat model in DFM inspired by the Western Scheldt Estuary in the Netherlands, based on the domain presented in Bij de Vaate et al. (2020). Our domain consists of a flat bed with a slope of 0.0016 m/m, 2,000-m length in cross-shore direction and 700 m width in alongshore direction. We used a rectangular grid with 20-m grid spacing below

https://doi.org/10.5194/egusphere-2026-3337
Preprint. Discussion started: 16 July 2026

the 0-m elevation mark (left part of domain, Fig. S1), and 10-m spacing above 0 m. We ran DYCOVE-DFM with a simplified M2-tide of 3-m tidal range and 12-hour period, 12 coupling intervals per ecological year at 24 hours each (two tidal periods per coupling interval), and a MORFAC/ECOFAC of 30. We modelled 10 years of eco-morphodynamic change to study channel initiation and establishment of three pioneer marsh species that represent the gradient from low- to high-intertidal vegetation in northwestern Europe (Van der Wal et al., 2008; De Vriend et al., 2011; Bij de Vaate et al., 2020): *Salicornia procumbens* (Salicornia), *Spartina anglica*, an invasive species in the Netherlands, (Spartina), and *Puccinellia maritima* (Puccinellia). We modelled all three species in conjunction and compared the resulting vegetation cover and seasonality with data from satellite imagery in a saltmarsh in the Netherlands using the Normalized Difference Vegetation Index (NDVI). We then modelled a second scenario excluding Spartina to compare our results with a non-invasion scenario.

The NDVI represents a proxy of relative vegetation biomass that can identify vegetation seasonality (Eastman et al., 2013). We assess two types of vegetation dynamics: 1) seasonal patterns for temperate marshes with high and low biomass in the summer and winter, respectively, (van der Wal et al., 2008) and 2) the development of species zonation for an invasive and non-invasive species scenario described in Nehring & Hesse (2008). Figure 2 compares vegetation cover for winter and summer for the three-species simulation compared with NDVI maps of the Saeftinghe marsh, a mature marsh in the inner part of the lower Western Scheldt Estuary, averaged for the months of February and August 2020-25, respectively. The NDVI maps show a transition from lower to higher biomass with distance from the channel (blue) for both seasons, representing typical zonation in temperate marshes (Van Belzen et al., 2017). Overall summer biomass is higher than in the winter. Bare tidal channel fringes in the winter are colonized with sparse vegetation cover in the summer indicating vegetation cover of an annual species (e.g., Salicornia). The idealized tidal flat model shows the same pattern for the respective ETS of 2 (February) and 8 (August): vegetation volume per m^2 (the product of stem density, height, and cross-sectional area) increases with distance from the main channel in both seasons with winter volume being lower than in the summer (Fig. 2e, f).

https://doi.org/10.5194/egusphere-2026-3337
Preprint. Discussion started: 16 July 2026

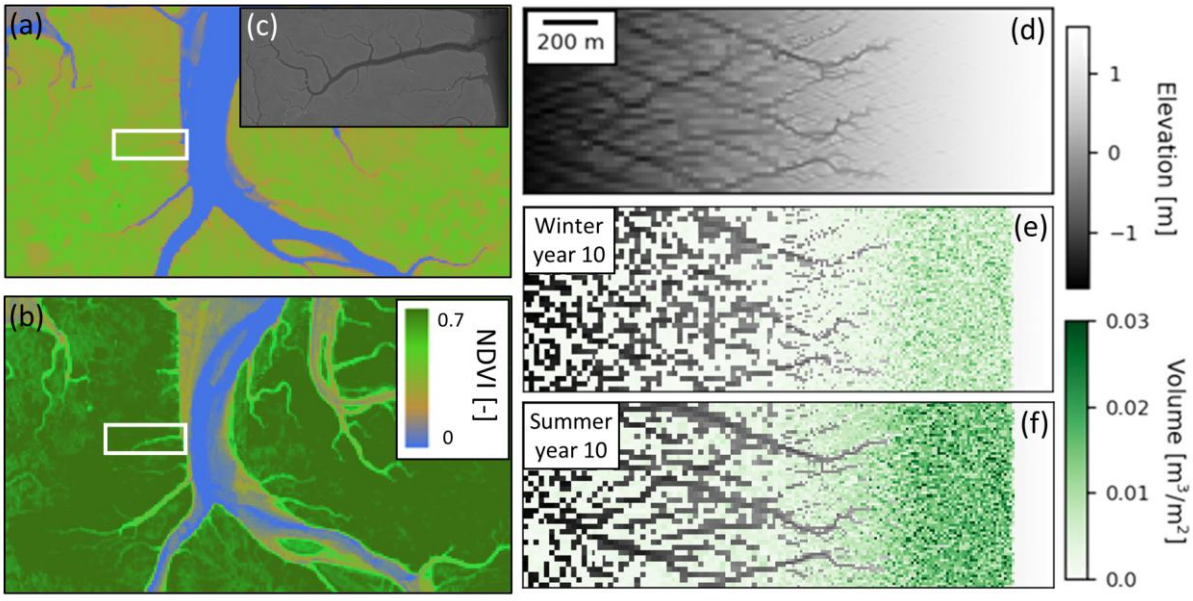

Figure 2: (a) Normalized Difference Vegetation Index (NDVI) in the Saeftinghe marsh, the Netherlands, averaged for February and (b) August 2020-2024. (c) shows bed level data of a selected region (white rectangles in (a) and (b); Dutch Water Authorities; https://www.ahn.nl, accessed June 1, 2026), showing typical marsh channel shape. DYCOVE-DFM model results are presented in (d) final bathymetry in year 10, (e) total combined vegetation volume for the three species run for the winter and (f) the summer on the tidal flat with an evolving tidal channel network. Note that the midpoint of the model domain represents the mid-intertidal zone and breakpoint between lower and higher grid resolution.

We compare zonation patterns with data presented in König (1948) and Nehring & Hesse (2008), which report a transition in the dominant species on tidal tidal flats in Northwestern Europe with the introduction of *Spartina anglica* after 1920. In the absence of Spartina, low tidal elevations were dominated by Salicornia and higher elevations by Puccinellia. After Spartina was introduced, it colonized both high and low intertidal marsh elevations, where it dominated over the two native species. The model results show good agreement with these observations (Fig. 3a-d). In the three-species scenarios, Spartina is dominant across most of the elevations from the centre to higher tidal flat (Fig. 3a, b). Only in areas where highest inundation occurs, Salicornia, a flood-tolerant species, dominates large areas. In the control run without Spartina (Fig. 3c, d), both Salicornia and Puccinellia have higher coverage in higher intertidal elevations. Especially Puccinellia can colonize a much greater portion of the upper intertidal zone than under competitive pressure from Spartina.

https://doi.org/10.5194/egusphere-2026-3337
Preprint. Discussion started: 16 July 2026

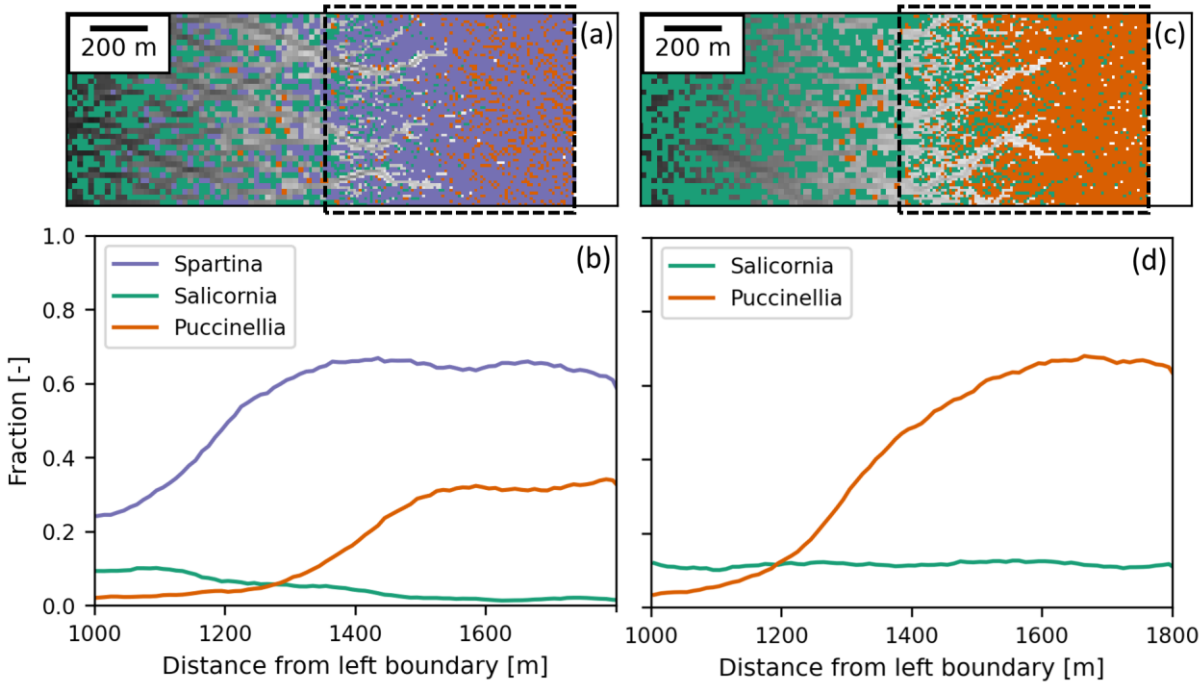

Figure 3: (a, c) Maps of the dominant species fraction in the DYCOVE-DFM tidal flat model for the simulations with and without Spartina. (b, d) Averaged species fraction over the domain above mean water with distance from the ocean boundary (dashed box in (a) and (b)).

3.2 Vegetation predictions in a hydrodynamic delta model in ANUGA

To assess model performance on a realistic coastal bathymetry, we modelled vegetation establishment and expansion of two species in a hydrodynamic simulation of Wax Lake Delta (WLD), a river-dominated, microtidal delta in the Gulf of Mexico, Louisiana. The ANUGA model was created using a topo-bathymetry dataset from 2016 that was used for a calibrated model presented in Wright et al. (2022) (Fig. S2). We used an unstructured mesh with an average element edge length of ≈40 m in active areas within the delta and an average spacing of 300 m in the bay. We applied a diurnal tidal boundary condition with a tidal period of 24 hours and an amplitude of 0.2 m (Rovai et al., 2022) at a mean sea level of 0.26 m (Wright et al., 2022). For the upstream discharge boundary, we developed a synthetic bi-modal annual hydrograph based on average high and low discharge values in WLD based on gauge timeseries (Fig. S2a). The hydrograph was scaled to the ecological modelling time such that each hydrograph cycle occurs once per ecological year. Similar as in Set 1, we modelled 12 couplings per year with an ETS of 24 hours using an ECOFAC of 30, resulting in a hydrodynamic simulation time of 12 days per ecological year. Sensitivity of the hydrodynamics and predicted vegetation cover was assessed for ECOFACs of 15 and 60, which showed only minor variations in vegetation distributions (Fig. S3).

Using DYCOVE, we modelled two generic marsh species in WLD based on the high intertidal species *Colocasia esculenta* (Colocasia) and the low intertidal species *Nelumbo lutea* (Nelumbo). While many of the parameters used to parameterize

https://doi.org/10.5194/egusphere-2026-3337
Preprint. Discussion started: 16 July 2026

Colocasia and Nelumbo are based on values from the literature (Table S1), we use these species to represent more generally a high intertidal species and low intertidal species, respectively, as they are two of the most dominant species (Jensen et al., 2021). We acknowledge that there are many more species present in WLD that are not included in our analyses. For example, although Colocasia colonizes supratidal zones in WLD, its abundance varies based on distance from the delta apex, with the levees on the more upstream islands having substantial riparian tree growth (Rovai et al., 2022). Although Wax Lake Delta is partly colonized by subtidal vegetation in delta islands (Rovai et al., 2022), DYCOVE is not designed to represent permanently submerged vegetation and therefore those vegetation types are not considered here.

We used colonization scheme (1) for Nelumbo, which identifies all grid cells that were both wet and dry as suitable for colonization, and scheme (3) for the higher intertidal/supratidal vegetation type Colocasia, which identifies all cells that were dry or partly dry as suitable for colonization. Colonization occurred during ETS 2-4, mimicking seed dispersal and rhizomal expansion throughout the growth period between February and May. Mortality thresholds were loosely based on average inundation parameters reported from Wax Lake Delta (Rovai et al., 2022) (Table S1). For both species, the initial colonization fraction is 0.3 to mimic gradual colonization, and establishment probability is 100%. We modelled vegetation dynamics over a five-year ecological period (i.e., five hydrograph cycles) as this time was sufficient to produce a stable vegetation cover with similar seasonal dynamics.

We assess model performance based on cell-to-cell comparisons with hydrogeomorphic zones presented in Rovai et al. (2022) to count correctly and incorrectly predicted vegetated/unvegetated cells and correctly and incorrectly predicted vegetation species locations. Hydrogeomorphic zones are based on bed elevations and represent static thresholds primarily used to distribute vegetation in calibrated hydro-(morpho)dynamic models (e.g., in Wright et al., 2022) or to predict species distributions (Jensen et al., 2021). We compare our process-based approach to these static thresholds to assess how well dynamic models can reproduce widely accepted species allocation (Fig. 4a). We construct a confusion matrix based on this comparison counting the number of true positives (TP), false positives (FP), and false negatives (FN, i.e., predicted bare soil instead of vegetation) and compute precision (eq. S1), recall (eq. S2), and F1 score (eq. S3) to quantify the model's performance. Precision measures the positive predictive value, meaning the probability that a positive prediction reflects a true positive condition. Recall measures the completeness of positive detection, meaning the probability of correctly identifying a positive instance given that it is truly positive. The F1 score represents the harmonic mean of the two. We did not consider true negatives, as we assumed that all intertidal and supratidal cells in the delta are vegetated.

The DYCOVE-ANUGA model reproduces both vegetated and unvegetated delta islands as well as the observed zonation patterns from high to low elevation (Fig. 4). Figure 4b shows that vegetation establishes along island levees and higher elevations in the island interior (supratidal and upper intertidal in Fig. 4a) with a realistic vegetation zonation driven by the inundation and desiccation gradients: Colocasia grows at higher elevations along island margins and Nelumbo adjacently at upper and lower intertidal elevations towards the inner islands.

The results from the confusion matrix show a high predictive capability for vegetated and unvegetated cells with an F1-score of 0.81 (Fig.4c). The high precision value indicates that few subtidal cells were colonized by vegetation in DYCOVE.

https://doi.org/10.5194/egusphere-2026-3337
Preprint. Discussion started: 16 July 2026

However, the 0.7 for the model recall indicates that a larger area in the intertidal or supratidal zone was predicted without vegetation, which affects overall accuracy. Here, the predicted bare areas were mainly related to the lowest lying intertidal elevations that experience high die-off during the flood stage without subsequent recolonization.

Predictions of species-specific vegetation cover is variable with a very high accuracy for Colocasia (96%) and average accuracy for Nelumbo (40%) (Fig. 4d). We evaluate species-level cover under the assumption that Nelumbo grows only in the lower intertidal zone and Colocasia in the upper intertidal and supratidal zones (Fig. 4a, d), where we define predicted accuracy of each species as the number of cells where a species is in the correct location divided by the total number of predictions for that species. High accuracy for Colocasia indicates that it is almost always correctly predicted in either the upper intertidal zone or supratidal zone. Lower accuracy for Nelumbo indicates that it is often predicted outside of the lower intertidal zone, mainly in the upper intertidal zone. The overall accuracy of the model is close to 0.71%, meaning that 71% of the cells in the inter- and supratidal areas were colonized by the correct species in DYCOVE.

https://doi.org/10.5194/egusphere-2026-3337
Preprint. Discussion started: 16 July 2026

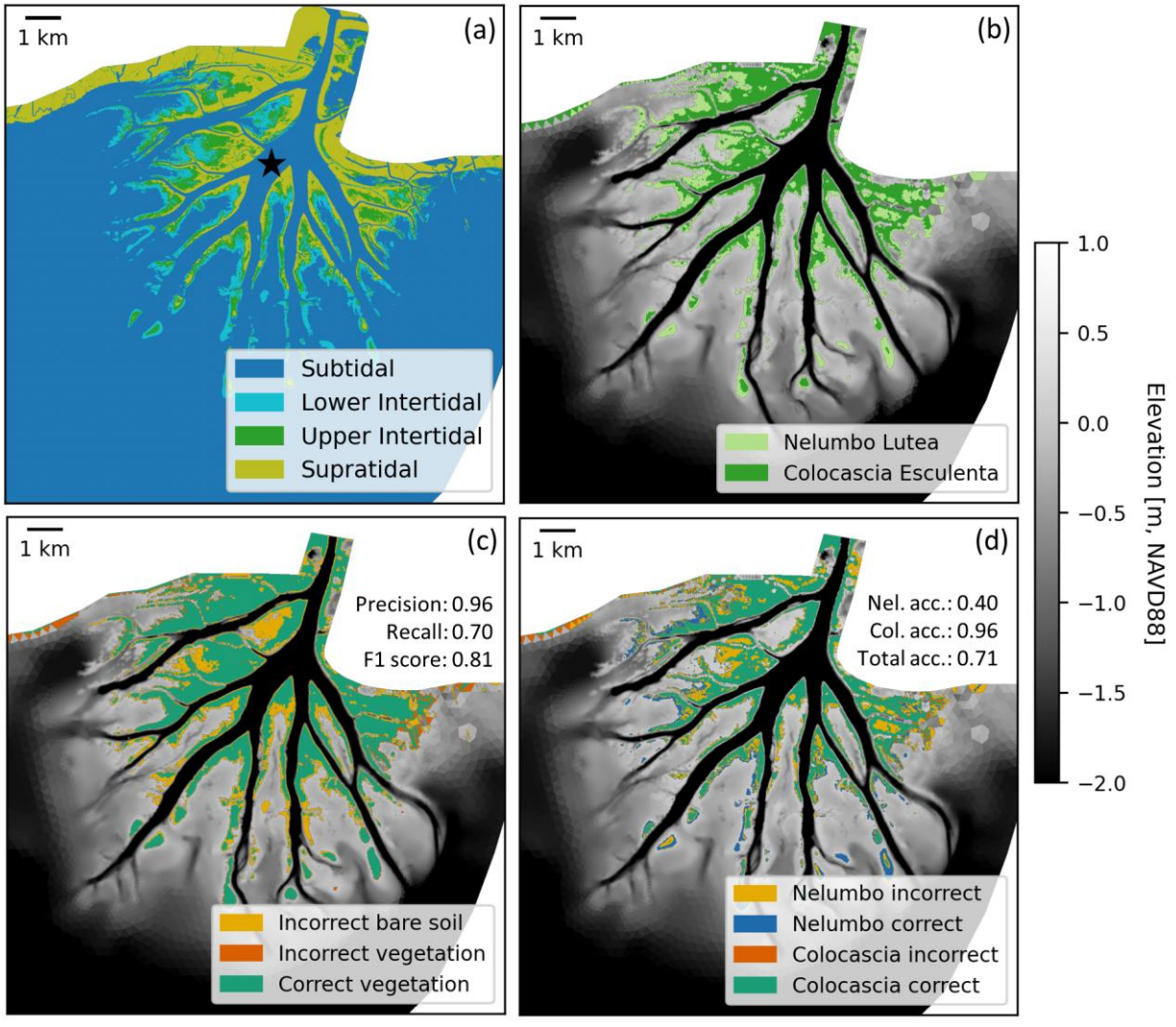

Figure 4: (a) Map of hydrogeomorphic zones as reported by Rovai et al. (2022) based on the comparison between bed elevation and average water surface elevations in the fall of 2021. Star denotes location of water levels presented in Fig. S3A. (b) Distribution of modelled vegetation types during ETS 8 (August). (c) Cell-wise comparison of correctly/incorrectly predicted vegetated and unvegetated cells during ETS 8 compared with zones shown in (a) with statistics. (d) Cell-wise comparison of correctly/incorrectly predicted vegetation types during ETS 8 compared with zones shown in (a) including accuracy calculations of correctly predicted cells for each species. Colocasia prediction is considered "correct" if it falls in the upper intertidal or supratidal zones in (a). Nelumbo prediction is considered "correct" if it falls in the lower intertidal zone in (a).

https://doi.org/10.5194/egusphere-2026-3337
Preprint. Discussion started: 16 July 2026

4 Discussion

4.1 Verification of species predictions and zonations

The dynamic vegetation model presented in Brückner et al. (2019) demonstrated that literature-based vegetation models can reproduce observed vegetation patterns qualitatively and quantitatively with approximately 60% accuracy based solely on ecological rules and without calibration. Their model depends on proprietary software and is coupled with Delft3D FLOW. Here we show that the successor model DYCOVE, which is open-source, well-documented, and coupled with the two H-M models DFM and ANUGA, was able to reproduce vegetation cover and zonation of multiple generic vegetation species on river- and tide-dominated domains with typical hydrodynamic forcings. DYCOVE reproduced species patterns and emergent tidal channel networks that are qualitatively similar to observations in northwestern Europe based on process-based equations and without parameter calibration (Fig. 2). The emergent tidal channel networks are a manifestation of the dynamic feedbacks that occur within the DYCOVE framework, capturing tidal channel emergence via preferential flow paths around vegetation patches that subsequently expand into mature marshes (Temmerman et al., 2007). With regard to ongoing research assessing the effects of species invasions on marsh communities and their subsequent biogeomorphic feedbacks, we show that DYCOVE is able to reproduce species distributions similar to observations from both native and invaded marsh communities (here limited to three species). Despite the lack of direct competition in DYCOVE, simple rules based on indirect competition for space incorporated by literature-based colonization characteristics (i.e., colonization timing and establishment probability) allow the model to reproduce the underlying behaviour of Spartina invasion observed in marshes in Northwestern Europe (Fig. 3c, d; Nehring & Hesse, 2008).

Using ANUGA to simulate supra- and intertidal vegetation establishment and growth in a river-dominated delta over a five-year period, DYCOVE was able to reproduce vegetated and unvegetated grid cells with a high F1 score of 0.81 (Fig. 4). When comparing correct species predictions, DYCOVE's accuracy was very high for Colocasia. This accuracy is likely linked to its wide habitat area, including the supratidal zone. It is highly unlikely that we would have falsely predicted Colocasia in this comparison, because we are assuming all tidal and supratidal zones are fully vegetated. The prediction on the lower intertidal Nelumbo, which has an accuracy of 40%, is mainly due to an overprediction in upper intertidal cells. According to the hydrogeomorphic zones, Nelumbo is mainly found in the lower intertidal, but can also penetrate intermediate elevations (Bevington et al., 2022). In addition, we imposed Nelumbo as the species that colonizes first, which allows it to occupy elevations where Colocasia might otherwise establish or outcompete Nelumbo. These two mechanisms can explain the overprediction of Nelumbo at higher elevations. Additionally, cold fronts and storms drive long-term vegetation cover and zonation (Bevington et al., 2017; 2022), which are not included in our model. However, given the model's simplifications induced by the hydrograph and the static bed level, DYCOVE shows a high success rate of matching elevation-based vegetation distributions (Wright et al., 2022; Rovai et al., 2022). While often used in hydro-(morpho)dynamic models, static thresholds cannot reproduce seasonal variability nor provide information on the mechanisms that determine vegetation pattern, a gap that DYCOVE can fill.

https://doi.org/10.5194/egusphere-2026-3337
Preprint. Discussion started: 16 July 2026

4.2 Sensitivity of results to important model assumptions

DYCOVE was translated from the MATLAB model that was validated in Brückner et al. (2019) and applied in several subsequent studies that showed that the model can reproduce generic saltmarsh establishment and growth in estuaries (Brückner et al., 2020; 2021) and in tidal basins (Boechat Albernaz et al., 2023) from literature-based parameterizations as well as establishment and zonation of multiple pioneer species on tidal flats (Bij de Vaate et al., 2020). We show that DYCOVE leads to similar results in DYCOVE-DFM simulations as in Bij de Vaate et al. (2020), validating the model implementation via the BMI including species seasonality and zonation (Fig. 3). In addition, we show that indirect species competition induces shifts in the species composition similar to reports from field observations (Nehring & Hesse, 2008), being able to represent broader species dynamics via simplified ecological rules. Below we focus on the new DYCOVE-ANUGA implementation, which advances the previous application to an implementation in ANUGA and shows the applicability in fluvially-influenced coastal areas. Our discussion and sensitivity simulations therefore focus mainly on those new features, including guidelines on the choice of parameter space relevant to models using unsteady boundary conditions.

4.2.1 Modelling vegetation establishment and mortality under quasi-steady and unsteady conditions

The dynamic vegetation model presented in Brückner et al. (2019) was validated for intertidal vegetation establishment and growth, where the tide is the main driver in hydrodynamic forcing. These conditions are valid in meso- and macrotidal environments that are sheltered from high wind waves as well as strong tidal anomalies due to seasonal river discharges, such as tide-dominated estuaries. Although the model was shown to reproduce vegetation in an H-M model forced by water levels from timeseries (Brückner et al., 2019), most models assume a constant or quasi-constant boundary condition and the colonization of vegetation might not occur in areas that depend on seasonal inundation, such as from spring-neap-tidal cycles or river inputs. To allow for broader colonization ranges, three additional colonization strategies were implemented in DYCOVE. These options allow for overcoming limitations in cases where the hydrodynamics are not variable enough to produce realistic vegetation cover over all elevation ranges, e.g., due to simplified boundary conditions or where establishment is also driven from rhizomes and wind-driven dispersal. The results from the DYCOVE-ANUGA simulation show that colonization strategy (1) is suitable for species that grow in intertidal elevations, whereas colonization strategy (3) or (4) are needed to distribute Colocasia on the highest bed elevations. These new colonization schemes are needed for two reasons. First, the topo-bathymetry in the WLD model is well-developed when first coupled with DYCOVE, leading to limited flooding (and therefore colonization under scheme (1)) of high elevations. In H-M models that build the morphology from an initial low flat bed, colonization strategy (1) is suitable to reproduce species cover and zonation (Fig. 3). Second, the colonization window needs to coincide with both high and low water levels to be able to distribute seeds along both high and low elevations. If colonization occurs only during a specific set of water levels in the hydrograph, colonization is limited to the elevations that are classified as intertidal under those conditions.

https://doi.org/10.5194/egusphere-2026-3337
Preprint. Discussion started: 16 July 2026

4.2.2 Implications of unsteady hydrodynamic boundary conditions

Simulations with unsteady boundary conditions create dependency of the mortality thresholds on timing and duration of floods or low water levels. Since vegetation mortality depends on flood duration, vegetation will die more intensely during periods of pronounced flooding (i.e., flooding that lasts for several ETS, such as the riverine spring flood in Fig. S3). Desiccation during low flows can lead to similar extensive die-off for drought-sensitive species. To parameterize vegetation resistance accordingly, maximum mortality thresholds are set to values larger than one, such that 100% inundation/desiccation does not remove the entire fraction (Fig. 1c; Table S1). This allows for limited mortality if high or low flows persist for several weeks or months (and hence ETS).

The results from the DYCOVE-ANUGA model highlight the challenge of identifying supra-, inter- and subtidal zones under variable discharge conditions in river-dominated systems with implications for predicting species-specific vegetation colonization and mortality (Fig. 4d). For example, under unsteady discharge, the supratidal zone in the fall (the timestep for our comparison) is larger and lower in elevation than during the spring flood. In fact, most of the elevations of WLD delta are inundated at maximum water levels (i.e., superposition of high discharge and high tide) (Wright et al., 2022), reducing the supratidal area as defined by hydrogeomorphic zones, which affects vegetation growth and zonation (Bevington et al., 2022). The example of Nelumbo in our DYCOVE ANUGA simulation illustrates this: the incorrectly predicted occurrence of Nelumbo in the upper intertidal zone can be explained by Nelumbo's colonization window occurring during high water conditions in the spring, when supratidal elevations experience inundation (Fig. S1). The same mechanism explains the lack of predicted vegetated cells at subtidal elevations. If colonization is restricted to timesteps during the spring flood, colonization of lower elevations that become subaerial only at low flow remain unvegetated, leading to lower Nelumbo cover toward the lower elevations. This mismatch between model results and the data is because hydrogeomorphic zones are static thresholds that result from an accumulation of varying hydrodynamic conditions over years that cannot be represented in models with averaged hydrodynamic forcings (either steady or unsteady). As a result, this comparison highlights the strong predictive capacity of DYCOVE as it can reproduce overall cover and species distribution with high accuracy, despite the limitations of the simplified unsteady boundary conditions.

4.2.3 Colonization as a proxy for rhizomatous growth

DYCOVE's colonization schemes represent several reproductive strategies, such as seed dispersal, seed banks, and rhizomatous growth. Although the latter two are not incorporated explicitly, they can be approximated by allowing for recolonization in each ETS during the growth period, corresponding to the window of decreasing discharge, even if the seed dispersal window has already passed. This allows for the continuous colonization of suitable grid cells until the maximum carrying capacity is met. The rhizomatous growth fraction cannot be set differently from the colonization fraction.

Rhizomatous growth is a dominant establishment strategy of perennial herbaceous species in Wax Lake Delta (Bevington et al., 2022). To test the sensitivity of the model to the respective timings of colonization and unsteady discharge, we test an

https://doi.org/10.5194/egusphere-2026-3337
Preprint. Discussion started: 16 July 2026

extension of the colonization window as a proxy for rhizomatous growth that allows for recolonization where vegetation temporarily died off during the growth period. Figure 5 shows a comparison map for a WLD simulation where the colonization window has been extended through ETS 9 (September). The results show a reduction in the number of cells that were previously predicted incorrectly as unvegetated (Fig. 4), leading to a better recall and increased F1 score. On the other hand, the precision of the model is reduced, as slightly more vegetation is now predicted incorrectly in the upper fringes of the subtidal zone (thin orange band in Fig. 5a). Although this analysis highlights the effect of colonization parameter choice on the dynamics of the vegetation distribution, the differences are minor and overall model predictions are mainly governed by the combined parameterization of all ecological parameters instead of by small variations of each. This exercise does, however, illustrate the flexibility of DYCOVE and how the input vegetation parameters can be leveraged to adapt a dynamic vegetation model to the system of interest.

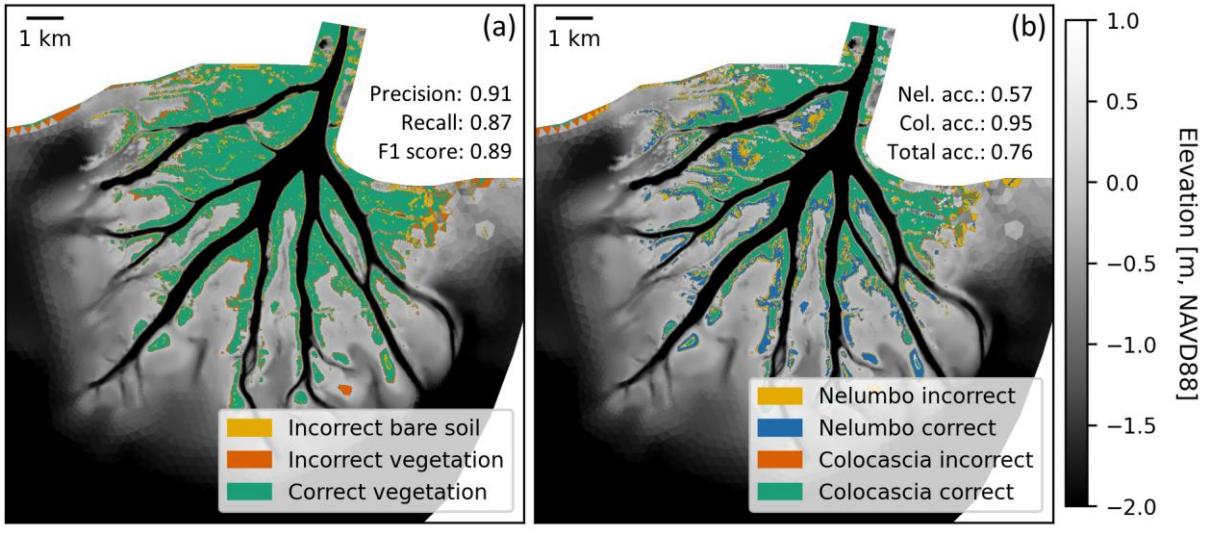

Figure 5: (a) Cell-wise comparison of correctly/incorrectly predicted vegetated and unvegetated cells during ETS 8 compared with zones shown in Fig. 4a including statistics. (b) Cell-wise comparison of correctly/incorrectly predicted vegetation types during ETS 8 compared with zones shown in Fig. 4a including accuracy calculations of correctly predicted cells for each species. Colocasia prediction is considered "correct" if it falls in the upper intertidal or supratidal zones. Nelumbo prediction is considered "correct" if it falls in the lower intertidal zone.

4.3 Limitations and future development

DYCOVE was developed to simulate intertidal vegetation dynamics. Processes that determine subtidal vegetation (e.g., water depth or optical conditions within the water) are outside the scope of the current implementation. DYCOVE assumes that vegetation growth depends mainly on inundation/desiccation periods. In addition, mortality due to flow velocities can cause uprooting and bed level changes that cause marsh erosion or burial. Those processes are important in dynamic coastal environments and for young and vulnerable vegetation and were shown to promote channel initiation and limit vegetation patch expansion on tidal flats (Temmerman et al., 2007; Bij de Vaate et al., 2020). Other habitat parameters, such as salinity,

https://doi.org/10.5194/egusphere-2026-3337
Preprint. Discussion started: 16 July 2026

nutrient supply or pollutants, are currently not included in DYCOVE. Our results show that DYCOVE can represent both vegetation that is driven by recurrent inundation by, for example, tides, as well as unsteady hydrodynamic conditions (Fig. 4). However, the user needs to be mindful of the timing and length of high and low flows and their scaling with the ecological time as described in Sect. 4.2.2. Currently, the ecosystem engineering effects included in DYCOVE are a direct hydraulic roughness and resulting indirect effects on sediment transport and erosion and deposition. Other relevant effects, such as an increase in cohesivity of the bed via roots or organic soil accretion from biomass production have not been implemented, yet. Ongoing developments include the implementation of organic accretion, which is particularly relevant in microtidal marshes (Nyman et al., 2006) and will enhance the predictive capabilities of DYCOVE.

5 Conclusions

The presented process-based coastal vegetation model DYCOVE is coupled with the hydrodynamic and hydro-morphodynamic models ANUGA and Delft3D Flexible Mesh. Using two test cases, we show that DYCOVE reproduces vegetation establishment, channel network development, and species zonation based on detailed ecological process rules. We further show that invasive species introduction can reproduce qualitative species shifts observed in the field through indirect competitive interactions alone. In a delta model with unsteady river discharge, prediction of both vegetation cover and species occurrence is high with an F1 score above 0.80 and total accuracy for species predictions exceeding 70%, despite simplifications in the hydrograph via an ecological scaling approach. The success of DYCOVE in reproducing vegetation cover and biogeomorphic feedbacks across different coastal environments and species will allow for broad future applications in assessing both coastal and deltaic geomorphic change, including impacts on species dynamics and the reciprocal effects of species on geomorphology as well as species shifts under varying boundary conditions.

Code and data availability

The DYCOVE code, installation instructions and examples are published on GitHub (https://github.com/Ecomomo-lab/dycove-model/, version 0.2.0). The model results used for this manuscript are available on Zenodo at https://doi.org/10.5281/zenodo.20704624 (Tull and Brückner, 2026)

Interactive Computing Environment

The DYCOVE GitHub repository includes several examples for both ANUGA and DFM, including a DYCOVE-ANUGA example in Jupyter notebook with detailed annotations that can be run interactively using Google Colab. This notebook example is located in the examples/notebooks/ folder of the GitHub repository.

https://doi.org/10.5194/egusphere-2026-3337
Preprint. Discussion started: 16 July 2026

Author contributions

NT wrote the DYCOVE code, coupled the code with DFM and ANUGA, performed the tests and simulations and generated the figures. MZMB designed the model and prepared the manuscript. All authors edited the manuscript.

Competing interests

The authors declare that they have no conflict of interest.

Acknowledgements

We thank the Delta-X project team and Kyle Wright for releasing the 2016 topo-bathymetry of Wax Lake Delta and associated datasets that were useful to our model validation. We also thank Anderson Amaya-Saldarriaga for helpful discussions related to the parameterizations of the vegetation species in the Wax Lake Delta model. Portions of this research were conducted with high-performance computational resources provided by Louisiana State University (http://www.hpc.lsu.edu).

Financial support

This study was supported by the U.S. Department of the Treasury through the Louisiana Coastal Protection and Restoration Authority's Center of Excellence Research Grants Program under the Resources and Ecosystems Sustainability, Tourist Opportunities, and Revised Economies of the Gulf Coast States Act of 2012 (RESTORE Act) (Award **No. 1 RCEGR260007-01-01**). The statements, findings, conclusions, and recommendations are those of the authors and do not

https://doi.org/10.5194/egusphere-2026-3337
Preprint. Discussion started: 16 July 2026

necessarily reflect the views of the Department of the Treasury. Further support was provided by the Department of Civil and Environmental Engineering and the Center for Computation and Technology at Louisiana State University.

References

Adam, P.: Saltmarsh ecology, Cambridge University Press, 1993.

Baart, F. et al.: BMI implementation in Python, GitHub, https://github.com/openearth/bmi-python, 2022.

Baptist, M. J., Babovic, V., Rodríguez Uthurburu, J., Keijzer, M., Uittenbogaard, R. E., Mynett, A., and Verwey, A.: On inducing equations for vegetation resistance, J. Hydraul. Res., 45, 435–450, 2007.

Barbier, E. B., Hacker, S. D., Kennedy, C., Koch, E. W., Stier, A. C., and Silliman, B. R.: The value of estuarine and coastal ecosystem services, Ecol. Monogr., 81, 169–193, 2011.

Batker, D., de la Torre, I., Costanza, R., Day, J. W., Swedeen, P., Boumans, R., and Bagstad, K.: The threats to the value of ecosystem goods and services of the Mississippi delta, in: Perspectives on the restoration of the Mississippi Delta, Springer Netherlands, Dordrecht, 155–173, 2014.

Bevington, A. E., Twilley, R. R., and Sasser, C. E.: Deltaic floodplain wetland vegetation dynamics along the sediment surface elevation gradient and in response to disturbance from river flooding and hurricanes in Wax Lake Delta, Louisiana, USA, Geomorphology, 398, 108011, 2022.

Bevington, A. E., Twilley, R. R., Sasser, C. E., and Holm Jr, G. O.: Contribution of river floods, hurricanes, and cold fronts to elevation change in a deltaic floodplain, northern Gulf of Mexico, USA, Estuar. Coast. Shelf Sci., 191, 188–200, 2017.

Bij de Vaate, I., Brückner, M. Z. M., Kleinhans, M. G., and Schwarz, C.: On the impact of salt marsh pioneer species-assemblages on the emergence of intertidal channel networks, Water Resour. Res., 56, e2019WR025045, https://doi.org/10.1029/2019WR025045, 2020.

https://doi.org/10.5194/egusphere-2026-3337
Preprint. Discussion started: 16 July 2026

Boechat Albernaz, M., Brückner, M. Z. M., Van Maanen, B., Van Der Spek, A. J. F., and Kleinhans, M. G.: Vegetation reconfigures barrier coasts and affects tidal basin infilling under sea level rise, J. Geophys. Res. Earth Surf., 128, e2022JF006703, https://doi.org/10.1029/2022JF006703, 2023.

Brückner, M. Z., Braat, L., Schwarz, C., and Kleinhans, M. G.: What came first, mud or biostabilizers? Elucidating interacting effects in a coupled model of mud, saltmarsh, microphytobenthos, and estuarine morphology, Water Resour. Res., 56, e2019WR026945, https://doi.org/10.1029/2019WR026945, 2020.

Brückner, M. Z., Schwarz, C., van Dijk, W. M., van Oorschot, M., Douma, H., and Kleinhans, M. G.: Salt marsh establishment and eco-engineering effects in dynamic estuaries determined by species growth and mortality, J. Geophys. Res. Earth Surf., 124, 2962–2986, 2019.

Cassaway, A. F., Twilley, R. R., Rovai, A. S., and Snedden, G. A.: Patterns of marsh surface accretion rates along salinity and hydroperiod gradients between active and inactive coastal deltaic floodplains, Estuar. Coast. Shelf Sci., 301, 108757, 2024.

Coco, G., Zhou, Z., Van Maanen, B., Olabarrieta, M., Tinoco, R., and Townend, I.: Morphodynamics of tidal networks: Advances and challenges, Mar. Geol., 346, 1–16, 2013.

Cornacchia, L., van de Vijsel, R. C., van der Wal, D., Ysebaert, T., Sun, J., van Prooijen, B., and van de Koppel, J.: Vegetation traits and biogeomorphic complexity shape the resilience of salt marshes to sea-level rise, Commun. Earth Environ., 5, 658, 2024.

Costanza, R., d'Arge, R., De Groot, R., Farber, S., Grasso, M., Hannon, B., and Van Den Belt, M.: The value of the world's ecosystem services and natural capital, Nature, 387, 253–260, 1997.

Day, J., Anthony, E., Costanza, R., Edmonds, D., Gunn, J., Hopkinson, C., and White, J. R.: Coastal wetlands in the Anthropocene, Annu. Rev. Environ. Resour., 49, 105–135, 2024.

Deltares: D-Flow Flexible Mesh, User Manual, Version 2026.02, 2025.

De Vriend, H. J., Wang, Z. B., Ysebaert, T., Herman, P. M., and Ding, P.: Eco-morphological problems in the Yangtze Estuary and the Western Scheldt, Wetlands, 31, 1033–1042, 2011.

https://doi.org/10.5194/egusphere-2026-3337
Preprint. Discussion started: 16 July 2026

Dzimballa, S., Willemsen, P. W. J. M., Kitsikoudis, V., Borsje, B. W., and Augustijn, D. C. M.: Numerical modelling of biogeomorphological processes in salt marsh development: Do short-term vegetation dynamics influence long-term development?, Geomorphology, 471, 109534, 2025.

Eastman, J. R., Sangermano, F., Machado, E. A., Rogan, J., and Anyamba, A.: Global trends in seasonality of Normalized Difference Vegetation Index (NDVI), 1982–2011, Remote Sens., 5, 4799–4818, https://doi.org/10.3390/rs5104799, 2013.

Elsey-Quirk, T., Lynn, A., Jacobs, M. D., Diaz, R., Cronin, J. T., Wang, L., and Justic, D.: Vegetation dieback in the Mississippi River Delta triggered by acute drought and chronic relative sea-level rise, Nat. Commun., 15, 3518, 2024.

Finotello, A., D'Alpaos, A., Marani, M., and Bertuzzo, E.: A minimalist model of salt-marsh vegetation dynamics driven by species competition and dispersal, Front. Mar. Sci., 9, 866570, 2022.

Fischer, J. M., Reed-Andersen, T., Klug, J. L., and Chalmers, A. G.: Spatial pattern of localized disturbance along a southeastern salt marsh tidal creek, Estuaries, 23, 565–571, 2000.

Friedrichs, C. T. and Perry, J. E.: Tidal salt marsh morphodynamics: a synthesis, J. Coast. Res., SI 27, 7–37, 2001.

Gourgue, O., Belliard, J. P., Xu, Y., Kleinhans, M. G., Fagherazzi, S., and Temmerman, S.: Dense vegetation hinders sediment transport toward saltmarsh interiors, Limnol. Oceanogr. Lett., 9, 764–775, 2024.

Hariharan, J., Wright, K., and Passalacqua, P.: dorado: A Python package for simulating passive particle transport in shallow-water flows, J. Open Source Softw., 5, 2585, 2020.

Hutton, E. W. H., Piper, M. D., and Tucker, G. E.: The Basic Model Interface 2.0: A standard interface for coupling numerical models in the geosciences, J. Open Source Softw., 5, 2317, https://doi.org/10.21105/joss.02317, 2020.

Jensen, D., Cavanaugh, K. C., Simard, M., Christensen, A., Rovai, A., and Twilley, R.: Aboveground biomass distributions and vegetation composition changes in Louisiana's Wax Lake Delta, Estuar. Coast. Shelf Sci., 250, 107139, 2021.

Jones, C. G., Lawton, J. H., and Shachak, M.: Organisms as ecosystem engineers, in: Ecosystem management: Selected readings, Springer New York, New York, NY, 130–147, 1994.

https://doi.org/10.5194/egusphere-2026-3337
Preprint. Discussion started: 16 July 2026

König, D.: Spartina townsendii an der Westküste von Schleswig-Holstein, Planta, 36, 34–70, 1948.

Ma, H., Larsen, L. G., and Wagner, R. W.: Ecogeomorphic feedbacks that grow deltas, J. Geophys. Res. Earth Surf., 123, 3228–3250, 2018.

Morris, J. T., Cahoon, D. R., Callaway, J. C., Craft, C., Neubauer, S. C., and Weston, N. B.: Marsh equilibrium theory, in: 4th International Conference on Invasive Spartina, ICI-Spartina 2014, 67–71, 2016.

Mungkasi, S. and Roberts, S. G.: Validation of ANUGA hydraulic model using exact solutions to shallow water wave problems, J. Phys. Conf. Ser., 423, 012029, 2013.

Murray, A. B., Knaapen, M. A. F., Tal, M., and Kirwan, M. L.: Biomorphodynamics: Physical-biological feedbacks that shape landscapes, Water Resour. Res., 44, W11301, 2008.

Nehring, S. and Hesse, K. J.: Invasive alien plants in marine protected areas: the Spartina anglica affair in the European Wadden Sea, Biol. Invasions, 10, 937–950, 2008.

Nyman, J. A., DeLaune, R. D., Roberts, H. H., and Patrick, W. J.: Relationship between vegetation and soil formation in a rapidly submerging coastal marsh, Mar. Ecol. Prog. Ser., 96, 269–279, 1993.

Piercy, C. D., Charbonneau, B. R., Russ, E. R., and Swannack, T. M.: Examining the commonalities and knowledge gaps in coastal zone vegetation simulation models, Earth Surf. Process. Landf., 49, 24–48, 2024.

Ranasinghe, R., Swinkels, C., Luijendijk, A., Roelvink, D., Bosboom, J., Stive, M., and Walstra, D.: Morphodynamic upscaling with the MORFAC approach: Dependencies and sensitivities, Coast. Eng., 58, 806–811, 2011.

Rovai, A. S., Twilley, R. R., Christensen, A., McCall, A., Jensen, D. J., Snedden, G. A., and Cavell, J. A.: Biomass allocation of tidal freshwater marsh species in response to natural and manipulated hydroperiod in coastal deltaic floodplains, Estuar. Coast. Shelf Sci., 268, 107784, 2022.

Sasser, C. E., Evers-Hebert, E., Holm Jr, G. O., Milan, B., Sasser, J. B., Peterson, E. F., and DeLaune, R. D.: Relationships of marsh soil strength to belowground vegetation biomass in Louisiana coastal marshes, Wetlands, 38, 401–409, 2018.

https://doi.org/10.5194/egusphere-2026-3337
Preprint. Discussion started: 16 July 2026

Schwarz, C., Gourgue, O., Van Belzen, J., Zhu, Z., Bouma, T. J., Van De Koppel, J., and Temmerman, S.: Self-organization of a biogeomorphic landscape controlled by plant life-history traits, Nat. Geosci., 11, 672–677, 2018.

Schwarz, C., Bouma, T. J., Zhang, L. Q., Temmerman, S., Ysebaert, T., and Herman, P. M. J.: Interactions between plant traits and sediment characteristics influencing species establishment and scale-dependent feedbacks in salt marsh ecosystems, Geomorphology, 250, 298–307, 2015.

Temmerman, S., Horstman, E. M., Krauss, K. W., Mullarney, J. C., Pelckmans, I., and Schoutens, K.: Marshes and mangroves as nature-based coastal storm buffers, Annu. Rev. Mar. Sci., 15, 95–118, 2023.

Tull, N. and Brückner, M. Z. M.: Model files for "Modelling dynamic coastal vegetation establishment and ecosystem engineering in hydro-morphodynamic models with DYCOVE", Zenodo, https://doi.org/10.5281/zenodo.20704624, 2026.

Vahsen, M. L., Todd-Brown, K. E. O., Hicks, J., Pilyugin, S. S., Morris, J. T., and Holmquist, J. R.: Cohort marsh equilibrium model (CMEM): History, mathematics, and implementation, J. Geophys. Res. Biogeosci., 129, e2023JG007823, https://doi.org/10.1029/2023JG007823, 2024.

Van Belzen, J., Van De Koppel, J., Kirwan, M. L., van Der Wal, D., Herman, P. M., Dakos, V., and Bouma, T. J.: Vegetation recovery in tidal marshes reveals critical slowing down under increased inundation, Nat. Commun., 8, 15811, 2017.

Van der Wal, D., Wielemaker-Van den Dool, A., and Herman, P. M.: Spatial patterns, rates and mechanisms of saltmarsh cycles (Westerschelde, The Netherlands), Estuar. Coast. Shelf Sci., 76, 357–368, 2008.

Van Oorschot, M., Kleinhans, M., Geerling, G., and Middelkoop, H.: Distinct patterns of interaction between vegetation and morphodynamics, Earth Surf. Process. Landf., 41, 791–808, 2016.

Wei, Y., van Maanen, B., Xie, D., Jiang, Q., Zhou, Z., and Schwarz, C.: Mangrove-saltmarsh ecotones: Are species shifts determining eco-morphodynamic landform configurations?, Earth's Future, 12, e2024EF004990, https://doi.org/10.1029/2024EF004990, 2024.

Wright, K., Hariharan, J., Passalacqua, P., Salter, G., and Lamb, M. P.: From grains to plastics: Modeling nourishment patterns and hydraulic sorting of fluvially transported materials in deltas, J. Geophys. Res. Earth Surf., 127, e2022JF006769, https://doi.org/10.1029/2022JF006769, 2022.